Published in final edited form as:
J Cell Physiol. 2012 May ; 227(5): 2022–2029. doi:10.1002/jcp.22931.

Essential role of ubiquitin C-terminal hydrolases UCHL1 and UCHL3 in mammalian oocyte maturation

Namdori R. Mtango[1], **Miriam Sutovsky**[3,4], **Catherine A. VandeVoort**[5], **Keith E. Latham**[1,2], and **Peter Sutovsky**[3,4,6]

[1]The Fels Institute for Cancer Research and Molecular Biology, Philadelphia, PA 19140

[2]Department of Biochemistry, Temple University, Philadelphia, PA 19140

[3]Division of Animal Sciences, University of Missouri-Columbia, Columbia, MO 65211-5300

[4]Department of Obstetrics, Gynecology and Women's Health, University of Missouri-Columbia, Columbia, MO 65211-5300

[5]California National Primate Research Center and Department of Obstetrics and Gynecology, School of Medicine, University of California, Davis, California 95616

Abstract

Ubiquitin C-terminal hydrolases (UCHs) comprise a family of deubiquitinating enzymes that play a role in the removal of multi-ubiquitin chains from proteins that are posttranslationally modified by ubiquitination to be targeted for proteolysis by the 26S proteasome. The UCH-enzymes also generate free monomeric ubiquitin from precursor multi-ubiquitin chains and, in some instances, may rescue ubiquitinated proteins from degradation. This study examined the roles of two oocyte-expressed UCHs, UCHL1 and UCHL3 in murine and rhesus monkey oocyte maturation. The *Uchl1* and *Uchl3* mRNAs were highly expressed in GV and MII oocytes, and were associated with the oocyte cortex (UCHL1) and meiotic spindle (UCHL3). Microinjection of the UCH-family enzyme inhibitor, ubiquitin-aldehyde (UBAL) to GV oocytes prevented oocyte meiotic progression beyond metaphase I in a majority of treated oocytes and caused spindle and first polar body anomalies. Injection of antibodies against UCHL3 disrupted oocyte maturation and caused meiotic anomalies, including abnormally long meiotic spindles. A selective, cell permeant inhibitor of UCHL3, 4, 5, 6, 7-Tetrachloroidan-1, 3-dione also caused meiotic defects and chromosome misalignment. Cortical granule localization in the oocyte cortex was disrupted by UBAL injected after oocyte maturation. We conclude that the activity of oocyte UCHs contributes to oocyte maturation by regulating the oocyte cortex and meiotic spindle.

Keywords

oocyte; ubiquitin; proteasome; UCH

[6]Correspondence: University of Missouri-Columbia, Columbia, MO 65211-5300; SutovskyP@missouri.edu.

INTRODUCTION

Sexual reproduction depends upon meiosis for the generation of haploid gamete nuclei, which unite after fertilization to form the diploid zygote. Oocyte meiotic maturation is defined by the transition between diakinesis and metaphase of meiosis II and requires nuclear envelope breakdown, rearrangement of the cortical cytoskeleton, and meiotic spindle assembly amongst other processes. Meiotic maturation produces an oocyte for fertilization. Regulated protein degradation is believed to be essential for oocyte maturation (Dekel, 2005; Josefsberg et al., 2000).

Covalent attachment of ubiquitin (Ub) chains to proteins, termed multi-ubiquitination or poly-ubiquitination, is a key regulatory mechanism in the substrate-specific, proteasomal degradation/recycling of proteins in animal and human cells [reviewed by (Hershko and Ciechanover, 1998)]. Protein ubiquitination is reversible via ubiquitin deconjugation (deubiquitination), performed by specific cysteine proteases and metalloproteases termed deubiquitinating enzymes (DUBs). Deubiquitination plays important roles in regulating Ub-dependent pathways. DUBs associated with the 19S proteasomal regulatory complex catalyze the removal of multi-ubiquitin chains from Ub-conjugated substrate proteins prior to substrate degradation in the 20S proteasomal core. DUBs also rescue substrate proteins from proteasomal degradation and recycle ubiquitin from multi-ubiquitin chains (Ventii and Wilkinson, 2008). Some DUBs perform ‘editing’ functions that control the fidelity of the Ub-conjugation process, preventing inappropriate degradation of cellular proteins [Reviewed in (Chung and Baek, 1999; Wing, 2003). The DUBs function by direct or indirect association with the proteasome, and also in the processing of Ub-precursor chains and Ub-adducts. DUBs also control protein trafficking in the cell (Nikko and Andre, 2007).

One class of DUBs, the JAMM domain proteins (e.g. proteasomal subunit PSMD14), is zinc metalloproteases (Ambroggio et al., 2004). Other DUBs are cysteine proteases, sensitive to inhibition by thiol reagents, such as N-ethylmaleimide and ubiquitin-aldehyde. These classical DUBs (cysteine proteases) fall into four distinct families: Ub-C-terminal hydrolases (UCHs), Ub-specific proteases (UBPs), otubain proteases (OTUs) and Machado-Joseph disease proteases (MJDs) (Ventii and Wilkinson, 2008). UCHs play a role in eliminating small adducts from ubiquitinated proteins, generating free monomeric Ub from its precursors, and removing ubiquitin from peptides and small proteins. The UBPs have a broader specificity, with some members of this family involved in deubiquitinating full length, intact proteins (Baarends et al., 1999).

The components of the complex ubiquitin system show remarkable evolutionary conservation, from yeast to mammals (Glickman and Ciechanover, 2002). There are recurring biological themes in the regulation of protein translation and protein clearance during meiosis, conserved between species and between sexes. However, unique differences could exist between mammalian species and between taxa with regard to gametic ubiquitin-proteasome pathway. Due to ethical constraints, a non-human primate model is the best choice for understanding how UCHs function in humans. Proper expression of DUBs and other components of ubiquitin system determine the developmental potential of primate zygotes/embryos (Mtango and Latham, 2007). Among the UCH-family DUBs, UCHL1 and

UCHL3 are the most highly expressed members in mammalian oocytes (Ellederova et al., 2004; Sekiguchi et al., 2006; Yi et al., 2007b). However, the mechanisms by which these DUBs control gamete maturation, fertilization and preimplantation development are largely unknown. The objective of the present study was to examine the expression of UCHs in murine and rhesus monkey oocytes and identify specific functions of these proteins during mammalian oogenesis, with special focus on oocyte maturation.

MATERIALS AND METHODS

Oocyte collection and in vitro maturation

Mouse oocytes—Germinal vesicle (GV)-stage oocytes were collected from ovaries of B6D2F1 mice at 44-46 h after the females were injected intra-peritoneally (i.p) with 5 IU Gonadotropin Pregnant Mare Serum (PMSG; Calbiochem, San Diego, CA). GV-intact follicular oocytes were released from the large antral follicles by puncturing with a needle in HEPES-buffered M2 medium supplemented with 0.1 mM of 3-isobutyl-1-methyl-xanthine (IBMX; Sigma-Aldrich, St. Louis, MO). All cultures were maintained in MEM-α medium supplemented with 10% FBS (Invitrogen Life Technologies/Gibco, Carlsbad, CA) at 37°C in a humidified atmosphere of 5% CO_2.

Rhesus monkey oocytes—Adult female rhesus macaques *(Macaca mulatta)* were housed at the California National Primate Research Center, as previously described (de Prada and VandeVoort, 2008). Females were observed daily for signs of vaginal bleeding, and the first day of menses was assigned Cycle Day 1. Beginning on Cycle Days 1–4, recombinant human FSH (r-hFSH; Organon, West Orange, NJ) was administered (37.5 IU) twice daily, intramuscularly for 7 days total. Cumulus-oocyte complexes (COCs) were collected on Day 8. Immature COCs were placed into 70 μl drops of M1A medium (Schramm et al., 2003). Only GV oocytes with at least two layers of cumulus cells were used in these experiments, because GV oocytes without cumulus will not mature. COCs were incubated in a humidified atmosphere of 5% CO_2 in air for 28–30 h at 37°C.

Inhibitors and antibody treatments—To study the roles of UCHL1 and UCHL3 in oocyte maturation we used several inhibitors (Ubiquitin aldehyde UBAL; Enzo/Biomol, Plymouth Meeting, PA UW 8450; UCHL3 inhibitor (EMD Biosciences/Calbiochem, Gibbstown, NJ: Cat # 662069) and antibodies specific to UCHL3. Ubiquitin aldehyde (UBAL; Enzo/Biomol, Plymouth Meeting, PA UW 8450) is not a pharmacological inhibitor, but a full length UBB protein in which the C terminus has been modified with an aldehyde-group. It is a highly potent; extremely stable inhibitor of ubiquitin-C-terminal hydrolases/ isopeptidases (Melandri et al., 1996). Approximately 5 pl of UBAL were injected at a concentration of 100 μM into GV oocytes to observe effect on oocyte maturation. A selective and potent UCHL3 inhibitor 4, 5, 6, 7-Tetrachloroidan-1, 3-dione, that exhibits ~125 fold greater selectivity for UCHL3 compared to UCHL1, was added during maturation or fertilization at the concentration of 100 μM. To study the roles of UCHL1 and UCHL3 in oocyte maturation, approximately 5 pl of 1μg/ μl of anti- UCHL3 antibody were injected into GV oocytes and matured in vitro. A non-immune rabbit/mouse serum was injected as a control. The specificity of antibodies was confirmed by Western blotting. To disrupt spindle

microtubules, GV stage oocytes were cultured in MEM-α medium containing 10μM nocodazole (Sigma, St. Louis, MO) for 16 h. After 16 h of maturation, the oocytes were collected, fixed for spindle examination by double labeling with anti-UCHL3 polyclonal antibody and anti-tubulin mouse monoclonal antibody E7 (Developmental Studies Hybridoma Bank, Iowa City, IA).

Quantitative RT-PCR, complementary cDNA Probes and hybridization—This was performed using a method for reverse transcription (RT) and exponential cDNA amplification that maintains the quantitative representation of the original mRNA population (Brady and Iscove, 1993; Iscove et al., 2002). The method incorporates a dot-blotting method, as described [(Mtango and Latham, 2007; Zheng et al., 2004) and www.preger.org]. The Primate Embryo Gene Expression Resource (PREGER) (www.preger.org) contains a collection of reverse transcribed and polymerase chain reaction (RT-PCR)-amplified cDNA libraries corresponding to more than 200 samples of mouse and rhesus monkey oocytes and preimplantation stage embryos. The oocytes and embryos were lysed in a modified RT buffer, followed by oligo(dT) annealing and processing through the RT step. After amplification, aliquots of each sample library were spotted onto filters by dot blotting. Complementary DNA probes were obtained by PCR from specific cDNA clone purchased from Open-Biosystems/Thermo Scientific (Huntsville, AL). [See Table 1 for primers list]. Primers without cDNA were used as negative control. Purified PCR products were then used for probe labeling as described (Zheng et al., 2004). Data were expressed as the mean count per minute (CPM) bound value (± standard error of the mean, SEM) for each stage/condition of oocytes and embryos included in the analysis. The statistical significance of differences was evaluated using the t-test ($P < 0.05$ considered significant).

Immunofluorescence—Oocytes were fixed and processed as described (Sutovsky et al., 2004; Yi et al., 2007a). A mix of anti-UCHL1 mouse IgG (ab20559, Abcam, Cambridge, MA; dil. 1/200) and affinity purified rabbit anti-UCHL3 IgG (LifeSpan Biosciences/MBL, Woburn, MA; LS-A8724; dil. 1/200) was applied overnight at 4°C, followed by washing and incubation for 40 min with a mixture of DAPI (blue DNA stain; Invitrogen/Life Technologies/Molecular Probes; 2.5 μg/ml), goat anti-rabbit-TRIC and goat anti-mouse IgG (red and green fluorescent, respectively; both from Zymed, San Francisco, CA, both diluted 1/100). Spindle localization of UCHL3 was confirmed by using an alternative rabbit anti-UCHL3 (Cat. #3525S; Cell Signaling Technology, Boston, MA). In some experiments, the fixed, permeabilized oocytes were stained with FITC-conjugated *Lens culinaris* agglutinin (LCA-FITC; Biomeda, Foster City, CA; dil. 1/100) to visualize cortical granules, or with rhodamine-phalloidin (Molecular Probes-Invitrogen, Carlsbad, CA) to label cortical actin microfilaments. Oocytes were mounted on slides in VectaShield medium and examined under a Nikon Eclipse 800 microscope equipped with a CoolSnap HQ CCD camera operated by MetaMorph 4.6 software. Negative controls were performed by replacing of specific antibodies with non-immune rabbit and mouse sera (Sigma, St. Louis MO) and these slides were photographed at comparable settings.

Western blotting—Western blotting was performed to detect the UCH proteins in oocyte lysates and to confirm antibody specificity (Burry, 2000). Zona free GV and metaphase-II

oocytes and zygotes (75 each) were used for western blotting. Protein lysates were prepared as described (Laemmli, 1970; Yi et al., 2007b), boiled, subjected to SDS-PAGE electrophoresis in 10% PAGE gels and blotted onto a PVDF membrane (Amersham, Piscataway, NJ). The membrane was blocked with Tris-buffered saline (TBS) containing 5% of non-fat dry milk for 1 h at room temperature. Incubations with anti-UCHL1 (Abcam Cambridge, MA, ab20559; dil. 1/1000) and anti-UCHL3 IgG (MBL, Woburn, MA; LS-A8724; dil. 1/500) were overnight at 4°C, followed by incubation in a horseradish peroxidase-conjugated anti-mouse or anti-rabbit (1:1000; Santa Cruz Biotech, Santa Cruz, CA) and enhanced chemiluminescent detection (Supersignal Pierce, Rockford, IL).

RESULTS

The mRNA and protein expression profile of mouse and rhesus monkey Uchl1 and Uchl3

The expression patterns of the mRNAs encoding UCHL1 and UCHL3 proteins were examined in mouse and rhesus monkey oocytes and embryos. Both mRNAs were expressed predominantly as maternal transcripts in both species, with lower expression during cleavage to the blastocyst stage (**Fig. 1 A - C**). In the mouse, *Uchl1* mRNA expression was low at the GV stage, and its apparent abundance increased at 22 h post hCG, followed by a decrease throughout later development (**Fig. 1 A)**. Absence of a decrease with α-amanitin treatment indicates that expression during the 1-cell stage is due to maternal mRNA. The mouse *Uchl3* mRNA showed an increase in apparent expression during oocyte maturation, indicating that it is probably polyadenylated and recruited for translation during this period [after GV-oocyte isolation the chromatin becomes condensed, rendering the oocyte transcriptionally inactive, but polyadenylation can enhance detection with oligo(dT) priming]. The *Uchl3* mRNA levels persisted after fertilization and during first embryo cleavage, decreased at the 2-cell stage, and remained steady thereafter (**Fig. 1 A**). This expression pattern validates mouse microarray results reported by (Zeng et al., 2004) (**Fig. 1 B**). Overall, these data indicate that both *Uchl1* and *Uchl3* mRNAs are highly expressed as maternal mRNAs in mouse oocytes and early embryos, and then persist at lower levels of expression during preimplantation development. In the rhesus monkey, *UCHL1* and *UCHL3* mRNA expression was high at the GV stage and decreased significantly during maturation (**Fig.1 C**). As with mouse, some zygotic polyadenylation and recruitment likely occurred, evident in the transcription-independent (α-amanitin insensitive) apparent increase in signal. The *UCHL3* mRNA was induced in blastocysts. The abundant expression of *Uchl1* and *Uchl3* genes in mouse oocytes was consistent with high levels of the corresponding proteins detected in the mouse oocyte extracts (**Fig. 1 D**).

Both rhesus monkey (**Fig. 2 A, B**) and mouse (**Fig. 2 C, D;** see also **Fig. 4 A**) oocytes showed a compartmentalized distribution of UCHs, with UCHL1 accumulating in the oocyte cortex and UCHL3 associating with the meiotic spindle. This localization of UCHL1 and UCHL3 proteins in the mouse and primate oocyte was similar to the patterns described in porcine and bovine oocyte (Yi et al., 2007b). Co-localization of UCHL3 with meiotic spindle microtubules was confirmed by double labeling with anti-tubulin antibody E7, by oocyte labeling with an alternative anti-UCHL3 antibody and by the dissipation of UCHL3 across the ooplasm following nocodazole treatment of maturing and mature oocytes (**Fig. 3**).

Such a treatment also induced dispersion of oocyte chromosomes and had an effect on the distribution of cortical granules in the oocyte cortex (**Suppl. Fig. 1 A-C**). The predominantly maternal expression of the *Uchl1* and *Uchl3* mRNAs in the oocytes and zygotes in both species, and probably polyadenylation and recruitment during maturation suggest important roles for the corresponding proteins in mature oocytes and early embryos.

The inhibition of ooplasmic UCHs alters the course of oocyte maturation

Strategies for examining the participation of UCHs in oocyte maturation included inhibition of UCH activity by microinjection of anti-UCH antibodies and non-cell-permeant UCH inhibitors (ubiquitin-aldehyde) into GV-stage oocytes, and culture with cell-permeant UCH-inhibitors in the IVM medium. Controls included injection of non-immune rabbit sera (NRS), vehicle solutions for cell-permeant inhibitors, and no injection.

Oocyte maturation in the presence of a specific UCHL3-inhibitor caused spindle abnormalities or a failure to complete GVBD in 52.6% of treated oocytes (**TABLE 2 A; Fig. 4 A-C**). Ubiquitin aldehyde (UBAL), a potent, specific inhibitor of all UCHs had an even more dramatic effect on oocyte maturation, with 88.3 ± 11.8% of UBAL-injected oocyte displaying abnormal or missing spindles and only 32% of oocytes reaching metaphase II, contrasting with 88 % MII-oocytes in vehicle-injected control (**TABLE 2 B; Fig. 4 D-G)**. A failure to undergo GV breakdown was often observed, or the oocyte chromatin underwent premature condensation (e.g. **Fig. 4 G**). A common anomaly in the UBAL-injected GV oocyte that reached metaphase II was an extremely large first polar body, in some cases bordering on symmetrical oocyte division (e.g. **Fig. 4 D**). The percentage of abnormal and missing spindles in the UBAL group was significantly higher ($P < 0.02$) compared to all other groups except the ones matured in the presence of UCHL3-inhibitor (52.6 ± 4.8 % abnormal/missing spindles; $P < 0.05$ compared to control groups; **TABLE 2 B; Fig. 4 H, I**). While there was a trend for increased incidence of spindle anomalies after anti-UCHL3 antibody injection (**Fig. 5; TABLE 2 C**), this increase was not statistically significant. Contrary to UBAL-injection, after which no progression beyond metaphase I was observed in most oocytes, the treatments targeting specifically UCHL3 were permissive for meiotic progression beyond metaphase I. Injection of anti-UCHL1 antibody did not alter spindle morphology or first polar body extrusion, but it did have a significant effect on sperm incorporation during fertilization [see *Companion Manuscript* by(Mtango et al., 2011)].

Measurements of spindle length and width in metaphase II oocytes exposed to UCH inhibiting substances that produced less subtle effects than UBAL revealed that GV oocyte injected with anti-UCHL3 antibody had significantly larger spindles compared to NS-injected oocyte, a pattern not unlike spindle elongation observed in mouse oocyte over-expressing the spindle-associated, guanine-dissociator protein LGN (Guo and Gao, 2009). Using the region statistics tool in MetaMorph (a relative measure of distance with no units), the average spindle pole width observed was significantly higher ($P=0.004$) in metaphase II oocyte pre-injected with anti-UCHL3 antibody (pole width of 53.6 ± 3.7) compared to NS-injected oocyte (39.0 ± 2.1) ($n=34$). Also, the average spindle length of anti-UCHL3 antibody injected oocyte (220 ± 10.4) was significantly larger ($P=0.008$) than that of NRS

injected oocyte (187.7 ± 8.9), control uninjected oocyte (192.0 ± 6.2)(n=57) and oocyte matured in the presence of UCHL3-inhibitor, which actually showed very short spindles (174.7 ± 6.3). Thus, inhibition of UCHs by UBAL and anti-UCH antibodies reduced the efficiency of normal oocyte maturation, and yielded defects in meiotic spindles.

Metaphase II Oocyte injection with UBAL alters cortical granule distribution

Because aberrant cortical granule (CG) migration was induced by UCH-inhibitors during bovine oocyte maturation (Susor et al., 2010), we examined whether the injection of mouse MII-oocytes with UBAL also had an effect on CG distribution. UBAL injection at the MII stage followed by 6 h culture caused a striking collar-shaped aggregation of CG adjacent to the CG-free area containing the oocyte spindle (**Fig. 6 A-C**). No such CG-rearrangement was observed in the MII oocyte exposed to inhibitors of UCHL3 (**Fig. 6 D**). Dual labeling with anti-UCHL1 antibody and lectin LCA-FITC to test whether UCHL1 was present within CGs or on their surface (**Suppl. Fig. 2**) revealed UCHL1 enrichment in the oocyte cortex harboring CGs, with no appreciable accumulation of UCHL1 inside CGs (**Suppl. Fig. 2 A, C**). Most likely, UCHL1 is associated with cytoskeletal elements (microfilaments, microtubules) controlling the movement of CGs in ooplasm and oocyte cortex. Such an association is consistent with the finding that the distribution of UCHL1 in the nocodazole-treated oocyte followed the redistribution of CGs and chromosomes (**Suppl. Fig. 2 B**).

DISCUSSION

We show here through multiple approaches that inhibition or loss of UCH function significantly interferes with normal oocyte maturation. Conserved oocyte expression of UCHL1 and UCHL3 in the mouse, (this study), pig (Yi et al., 2007b), cow (Susor et al., 2010; Yi et al., 2007b) and rhesus monkey (this study) indicates that these proteins likely play crucial roles across diverse species. We also show that the inhibitors and antibodies targeting oocyte UCHs have a profound negative effect on mouse oocyte maturation. Collectively, our data indicate that UCH functions are essential for critical processes in the oocyte maturation.

One of the major effects we observe is a negative effect of UCH inhibition on the formation of a normal meiotic spindle during oocyte maturation. Spindle lengths/pole-to-pole distances are altered and other attributes of the meiotic spindle, such as chromosome alignment, are disrupted. Such defects may lead to aneuploidy in the oocyte and resulting embryo. In addition to abnormal microtubule and chromosome organization within the meiotic spindle, the inhibition of spindle-associated UCHL3 also alters spindle pole-to-pole distance and spindle-pole width. The spindle pole-pole distance remains constant from metaphase to anaphase. The pole-to-pole distance of the metaphase spindle is reasonably constant in a given cell type; in the case of vertebrate female oocytes, this steady-state length can be maintained for substantial lengths of time, during which microtubules remain highly dynamic. Oocytes matured in poor conditions are more likely to have a shorter spindle length (long axis) and smaller spindle areas (Ueno et al., 2005). Although a number of molecular perturbations could influence spindle integrity (Doubilet and McKim, 2007; Guo and Gao, 2009; Schatten and Sun, 2009), a global understanding of the factors that

determine metaphase spindle length has not been achieved. The UCHs studied here may regulate germinal vesicle breakdown, spindle assembly, spindle pole focusing as well as ubiquitin-dependent cyclin degradation and chromosome segregation during metaphase-anaphase transition (Huo et al., 2006; Josefsberg et al., 2000; Susor et al., 2007; Yi et al., 2008). Also, we have observed meiotic spindle-colocalization of UCHL3 with separase/separin (Yanagida, 2005), an enzyme that may be a substrate of UCHL3 during mitotic metaphase-anaphase transition (PS; unpublished data). Ubiquitin-like protein NEDD8, a known substrate of UCHL3 has also been implicated in the control of spindle positioning and cell cycle progression during mitosis (Kurz et al., 2002).

The second major effect that we observed is on asymmetric cell division during meiosis. The inhibition of UCHs leads to excessively large polar bodies (PB), indicating a disruption in spindle localization or a dysfunction of microfilament cytoskeleton in the oocyte cortex. This may reflect another facet of defective spindle function and/or impaired cytoskeletal function in the oocyte cortex. The asymmetric oocyte division during meiosis is responsible for PB extrusion. Excessive allocation of cytoplasm and organelles to a polar body will without a doubt have a negative effect on fertilization and preimplantation embryo development. Polar body extrusion in the mouse is controlled by microtubules and actin microfilaments (Azoury et al., 2009). Putative factors controlling F-actin assembly during oocyte meiosis include microfilament associated proteins formin-2 (FMN2) and myosins (Schuh and Ellenberg, 2008), as well as ADP-ribosylation factor 1 [ARF1 (Wang et al., 2009)]. While we have not observed gross alteration of cortical microfilaments in the mouse oocytes subjected to UCH-inhibition, it is possible that the UCHs, and particularly oocyte-cortical UCHL1, affected the activity or turnover of the microfilament-regulating proteins. Examples of actomyosin turnover by ubiquitin-proteasome pathway (UPP) are well known (Cinnamon et al., 2009) and the formin-2-related proteins such as DIAPH3 are degraded by UPP during cell division (DeWard and Alberts, 2009). Proteasomal inhibitors increase poly-ADP ribosylation (Keller and Markesbery, 2000) which is dependent on ARF1 and other ARFs acting as stimulators of ADP-ribosyltransferase (Lee et al., 1992). Interestingly, expression of the mutated *Arf1* gene *(Arf1T31N)* causes mouse oocytes to cleave symmetrically instead of extruding the first PB during meiosis (Wang et al., 2009). The resultant pattern is reminiscent of UCH-inhibited oocytes seen in our studies. At least one of the ARF proteins, ARF6 appears to be regulated by ubiquitination (Yano et al., 2008), which could be reversed by UCHs. It is thus possible that UCHL1 and related UCHs may regulate actin and myosin-containing microfilaments during polar body extrusion.. The microfilament-controlled cytokinsesis, cleavage furrow formation and cell polarity establishment in the early embryos of *C. elegans* are controlled by ubiquitin C-terminal hydrolase CYK3 (Kaitna et al., 2002). The CYK-3 protein contains UCH domains homologous to mammalian ubiquitin-C-terminal hydrolases USP11 and USP32.

Altogether, our data demonstrate the importance of UCHL1 and UCHL3 in oocyte maturation. By applying specific inhibitors and antibodies, we have revealed the involvement of UCHL3 in the dynamics of oocyte meiotic spindle. Studies of UCHL1 hint at its role in first polar body extrusion and cortical granule positioning. Further efforts will

center on the identification of substrate proteins for these two UCHs in the mammalian oocytes.

Supplementary Material

Refer to Web version on PubMed Central for supplementary material.

ACKNOWLEDGEMENTS

This project was supported by National Research Initiative Competitive Grants no. 2007-35203-18274 and no. 2011-67015-20025 from the USDA National Institute of Food and Agriculture, to P.S., and grants from the National Center for Research Resources (RR15253, RR18907) and National Institute for Child Health and Human Development (HD41440, HD52788 and RR15253) to K.E.L. Additional funding was provided by the Food for the 21st Century Program of the University of Missouri-Columbia to P.S., grant RR-000169 (RR-13439) to C.A.V.

REFERENCES

Ambroggio XI, Rees DC, Deshaies RJ. JAMM: a metalloprotease-like zinc site in the proteasome and signalosome. PLoS Biol. 2004; 2(1):E2. [PubMed: 14737182]

Azoury J, Verlhac MH, Dumont J. Actin filaments: key players in the control of asymmetric divisions in mouse oocytes. Biol Cell. 2009; 101(2):69–76. [PubMed: 19076067]

Baarends WM, Roest HP, Grootegoed JA. The ubiquitin system in gametogenesis. Mol Cell Endocrinol. 1999; 151(1-2):5–16. [PubMed: 10411315]

Brady G, Iscove NN. Construction of cDNA libraries from single cells. Methods Enzymol. 1993; 225:611–623. [PubMed: 8231874]

Burry RW. Specificity controls for immunocytochemical methods. J Histochem Cytochem. 2000; 48(2):163–166. [PubMed: 10639482]

Chung CH, Baek SH. Deubiquitinating enzymes: their diversity and emerging roles. Biochem Biophys Res Commun. 1999; 266(3):633–640. [PubMed: 10603300]

Cinnamon Y, Feine O, Hochegger H, Bershadsky A, Brandeis M. Cellular contractility requires ubiquitin mediated proteolysis. PLoS One. 2009; 4(7):e6155. [PubMed: 19597551]

de Prada JK, VandeVoort CA. Growth hormone and in vitro maturation of rhesus macaque oocytes and subsequent embryo development. J Assist Reprod Genet. 2008; 25(4):145–158. [PubMed: 18278582]

Dekel N. Cellular, biochemical and molecular mechanisms regulating oocyte maturation. Mol Cell Endocrinol. 2005; 234(1-2):19–25. [PubMed: 15836949]

DeWard AD, Alberts AS. Ubiquitin-mediated degradation of the formin mDia2 upon completion of cell division. J Biol Chem. 2009; 284(30):20061–20069. [PubMed: 19457867]

Doubilet S, McKim KS. Spindle assembly in the oocytes of mouse and Drosophila--similar solutions to a problem. Chromosome Res. 2007; 15(5):681–696. [PubMed: 17674154]

Ellederova Z, Halada P, Man P, Kubelka M, Motlik J, Kovarova H. Protein patterns of pig oocytes during in vitro maturation. Biol Reprod. 2004; 71(5):1533–1539. [PubMed: 15229143]

Glickman MH, Ciechanover A. The ubiquitin-proteasome proteolytic pathway: destruction for the sake of construction. Physiol Rev. 2002; 82(2):373–428. [PubMed: 11917093]

Guo X, Gao S. Pins homolog LGN regulates meiotic spindle organization in mouse oocytes. Cell Res. 2009; 19(7):838–848. [PubMed: 19434098]

Hershko A, Ciechanover A. The ubiquitin system. Annu Rev Biochem. 1998; 67:425–479. [PubMed: 9759494]

Huo LJ, Zhong ZS, Liang CG, Wang Q, Yin S, Ai JS, Yu LZ, Chen DY, Schatten H, Sun QY. Degradation of securin in mouse and pig oocytes is dependent on ubiquitin-proteasome pathway and is required for proteolysis of the cohesion subunit, Rec8, at the metaphase-to-anaphase transition. Front Biosci. 2006; 11:2193–2202. [PubMed: 16720305]

Iscove NN, Barbara M, Gu M, Gibson M, Modi C, Winegarden N. Representation is faithfully preserved in global cDNA amplified exponentially from sub-picogram quantities of mRNA. Nat Biotechnol. 2002; 20(9):940–943. [PubMed: 12172558]

Josefsberg LB, Galiani D, Dantes A, Amsterdam A, Dekel N. The proteasome is involved in the first metaphase-to-anaphase transition of meiosis in rat oocytes. Biol Reprod. 2000; 62(5):1270–1277. [PubMed: 10775176]

Kaitna S, Schnabel H, Schnabel R, Hyman AA, Glotzer M. A ubiquitin C-terminal hydrolase is required to maintain osmotic balance and execute actin-dependent processes in the early C. elegans embryo. J Cell Sci. 2002; 115(Pt 11):2293–2302. [PubMed: 12006614]

Keller JN, Markesbery WR. Proteasome inhibition results in increased poly-ADP-ribosylation: implications for neuron death. J Neurosci Res. 2000; 61(4):436–442. [PubMed: 10931530]

Kurz T, Pintard L, Willis JH, Hamill DR, Gonczy P, Peter M, Bowerman B. Cytoskeletal regulation by the Nedd8 ubiquitin-like protein modification pathway. Science. 2002; 295(5558):1294–1298. [PubMed: 11847342]

Laemmli UK. Cleavage of structural proteins during the assembly of the head of bacteriophage T4. Nature. 1970; 227(5259):680–685. [PubMed: 5432063]

Lee CM, Haun RS, Tsai SC, Moss J, Vaughan M. Characterization of the human gene encoding ADP-ribosylation factor 1, a guanine nucleotide-binding activator of cholera toxin. J Biol Chem. 1992; 267(13):9028–9034. [PubMed: 1577740]

Melandri F, Grenier L, Plamondon L, Huskey WP, Stein RL. Kinetic studies on the inhibition of isopeptidase T by ubiquitin aldehyde. Biochemistry. 1996; 35(39):12893–12900. [PubMed: 8841133]

Mtango N, Sutovsky M, Susor A, Zhong Z, Latham KE, Sutovsky P. Essential role of maternal UCHL1 and UCHL3 in fertilization and preimplantation embryo development. Journal of Cellular Physiology. 2011 In press.

Mtango NR, Latham KE. Ubiquitin proteasome pathway gene expression varies in rhesus monkey oocytes and embryos of different developmental potential. Physiol Genomics. 2007; 31(1):1–14. [PubMed: 17550997]

Nikko E, Andre B. Evidence for a direct role of the Doa4 deubiquitinating enzyme in protein sorting into the MVB pathway. Traffic. 2007; 8(5):566–581. [PubMed: 17376168]

Schatten H, Sun QY. The role of centrosomes in mammalian fertilization and its significance for ICSI. Mol Hum Reprod. 2009; 15(9):531–538. [PubMed: 19549764]

Schramm RD, Paprocki AM, VandeVoort CA. Causes of developmental failure of in-vitro matured rhesus monkey oocytes: impairments in embryonic genome activation. Hum Reprod. 2003; 18(4): 826–833. [PubMed: 12660279]

Schuh M, Ellenberg J. A new model for asymmetric spindle positioning in mouse oocytes. Curr Biol. 2008; 18(24):1986–1992. [PubMed: 19062278]

Sekiguchi S, Kwon J, Yoshida E, Hamasaki H, Ichinose S, Hideshima M, Kuraoka M, Takahashi A, Ishii Y, Kyuwa S, Wada K, Yoshikawa Y. Localization of ubiquitin C-terminal hydrolase L1 in mouse ova and its function in the plasma membrane to block polyspermy. Am J Pathol. 2006; 169(5):1722–1729. [PubMed: 17071595]

Susor A, Ellederova Z, Jelinkova L, Halada P, Kavan D, Kubelka M, Kovarova H. Proteomic analysis of porcine oocytes during in vitro maturation reveals essential role for the ubiquitin C-terminal hydrolase-L1. Reproduction. 2007; 134(4):559–568. [PubMed: 17890291]

Susor A, Liskova L, Toralova T, Pavlok A, Pivonkova K, Karabinova P, Lopatarova M, Sutovsky P, Kubelka M. Role of ubiquitin C-terminal hydrolase-l1 in antipolyspermy defense of mammalian oocytes. Biol Reprod. 2010; 82(6):1151–1161. [PubMed: 20164442]

Sutovsky P, Van Leyen K, McCauley T, Day BN, Sutovsky M. Degradation of paternal mitochondria after fertilization: implications for heteroplasmy, assisted reproductive technologies and mtDNA inheritance. Reprod Biomed Online. 2004; 8(1):24–33. [PubMed: 14759284]

Ueno S, Kurome M, Ueda H, Tomii R, Hiruma K, Nagashima H. Effects of maturation conditions on spindle morphology in porcine MII oocytes. J Reprod Dev. 2005; 51(3):405–410. [PubMed: 15812143]

Ventii KH, Wilkinson KD. Protein partners of deubiquitinating enzymes. Biochem J. 2008; 414(2): 161–175. [PubMed: 18687060]

Wang S, Hu J, Guo X, Liu JX, Gao S. ADP-ribosylation factor 1 regulates asymmetric cell division in female meiosis in the mouse. Biol Reprod. 2009; 80(3):555–562. [PubMed: 19005166]

Wing SS. Deubiquitinating enzymes--the importance of driving in reverse along the ubiquitin-proteasome pathway. Int J Biochem Cell Biol. 2003; 35(5):590–605. [PubMed: 12672452]

Yanagida M. Basic mechanism of eukaryotic chromosome segregation. Philos Trans R Soc Lond B Biol Sci. 2005; 360(1455):609–621. [PubMed: 15897183]

Yano H, Kobayashi I, Onodera Y, Luton F, Franco M, Mazaki Y, Hashimoto S, Iwai K, Ronai Z, Sabe H. Fbx8 makes Arf6 refractory to function via ubiquitination. Mol Biol Cell. 2008; 19(3):822–832. [PubMed: 18094045]

Yi YJ, Manandhar G, Oko RJ, Breed WG, Sutovsky P. Mechanism of sperm-zona pellucida penetration during mammalian fertilization: 26S proteasome as a candidate egg coat lysin. Soc Reprod Fertil Suppl. 2007a; 63:385–408. [PubMed: 17566286]

Yi YJ, Manandhar G, Sutovsky M, Li R, Jonakova V, Oko R, Park CS, Prather RS, Sutovsky P. Ubiquitin C-terminal hydrolase-activity is involved in sperm acrosomal function and anti-polyspermy defense during porcine fertilization. Biol Reprod. 2007b; 77(5):780–793. [PubMed: 17671268]

Yi YJ, Nagyova E, Manandhar G, Prochazka R, Sutovsky M, Park CS, Sutovsky P. Proteolytic activity of the 26S proteasome is required for the meiotic resumption, germinal vesicle breakdown, and cumulus expansion of porcine cumulus-oocyte complexes matured in vitro. Biol Reprod. 2008; 78(1):115–126. [PubMed: 17942798]

Zeng F, Baldwin DA, Schultz RM. Transcript profiling during preimplantation mouse development. Dev Biol. 2004; 272(2):483–496. [PubMed: 15282163]

Zheng P, Patel B, McMenamin M, Reddy SE, Paprocki AM, Schramm RD, Latham KE. The primate embryo gene expression resource: a novel resource to facilitate rapid analysis of gene expression patterns in non-human primate oocytes and preimplantation stage embryos. Biol Reprod. 2004; 70(5):1411–1418. [PubMed: 14724133]

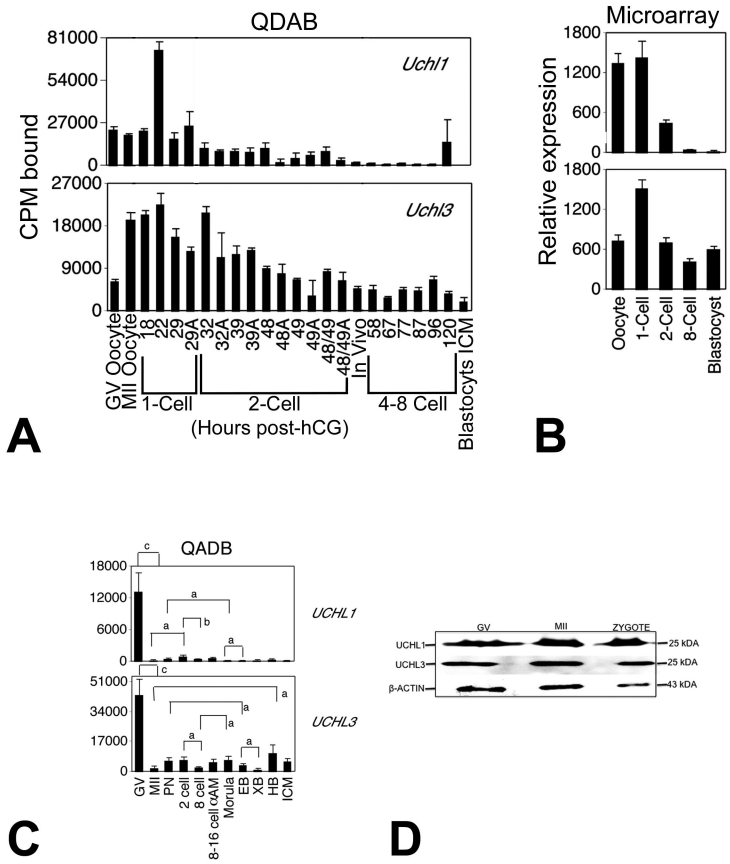

Fig. 1.

Expression profiles of *Uchl1* and *Uchl3* transcripts and proteins in mouse and rhesus monkey embryos. **A.** Mouse mRNA expression. The corresponding developmental stages, including germinal vesicle-intact oocyte (GVOOC), MII-stage oocyte (egg), 1-, 2-, 4-, and 8-cell stages, morula, and blastocyst, are indicated below the graph. The bar labeled “In Vivo” represents 2-cell stage embryos flushed from the oviduct and lysed without further culture. Numbers on the x-axis signify hours post hCG injection (induction of ovulation), corresponding to time at which the 1-8 cell embryos were collected. Hybridization signals were normalized to the amount of DNA bound to each dot and expressed in units of bound counts per minute (cpm) after conversion of phosphorimager data using a dot with a known quantity of ^{32}P for calibration. Bars indicate the mean value and SEM obtained for the stages or times indicated (between 3 and 8 samples per stage). **B.** Mouse UCH-expression data extracted from the microarray data deposited in the Gene Expression Omnibus repository (Zeng et al., 2004), which were obtained originally using the Affymetrix MOE 430A and 430B chip. The stages represented were GV-stage oocytes and embryos at the one-cell, two-cell, eight-cell, and blastocyst stages. These data were expressed as the mean (±SEM) Affymetrix array hybridization signals. **C:** Rhesus monkey mRNA expression data. Graphs show the relative levels of expression for GV- and MII-stage oocytes and pronuclear zygotes through hatched blastocyst stage embryos that were produced by *in vitro* fertilization of oocytes from hCG-stimulated females and then cultured in vitro in HECM9 medium; GV, germinal vesicle-stage oocyte; MII, MII-stage oocyte; PN, pronuclear one-cell

stage embryo; 2C, two-cell stage embryo; 8C, eight-cell stage embryo; 8–16C αAm, 8- to 16-cell stage cultured in a-amanitin; EB, early blastocyst; XB, expanded blastocyst; HB, hatched blastocyst. Expression data for the mRNAs encoding the indicated proteins are expressed as the mean counts per minute (CPM) bound, and the SEM is indicated. Statistically significant differences in gene expression corresponding to some of the major increases or decreases in expression are denoted by the brackets (for comparisons between stages at the ends of the brackets). **D.** Western blots of UCHL1 and UCHL3 in GV-stage mouse oocytes, MII oocytes and zygotes. Equal numbers of oocytes were used to prepare protein extracts for each sample/lane; β-actin served as a control.

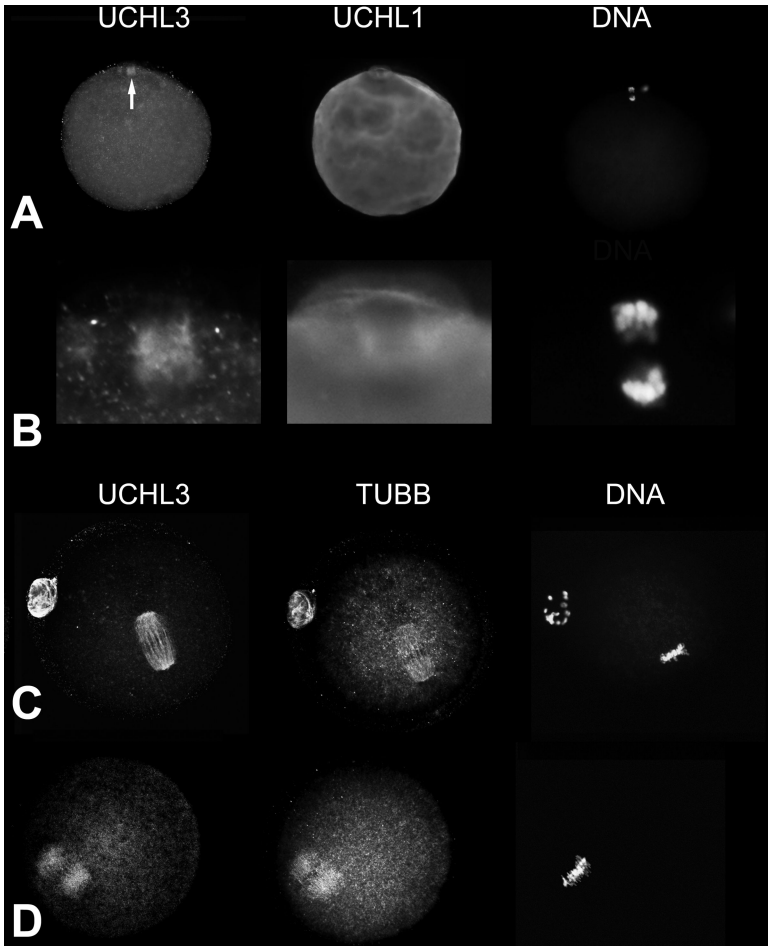

Fig. 2.

Association of UCHL3 with meiotic spindle in rhesus monkey (**A, B**) and mouse (**C, D**) oocytes. Oocyte DNA was counterstained with DAPI. **A.** Meiotic spindle-association of UCHL3 and cortical localization of UCHL1 in the rhesus monkey oocyte (telophase I). **B.** Detail of telophase spindle in an oocyte shown in panel A. **C.** Control MII mouse oocyte. **D.** Alternative antibody against UCHL3 confirmed spindle localization, overlapping with microtubule staining. Dual immunolabeling in panels A and B was performed with antibody against UCHL1 and with anti-tubulin (TUBB) antibody in panels C and D.

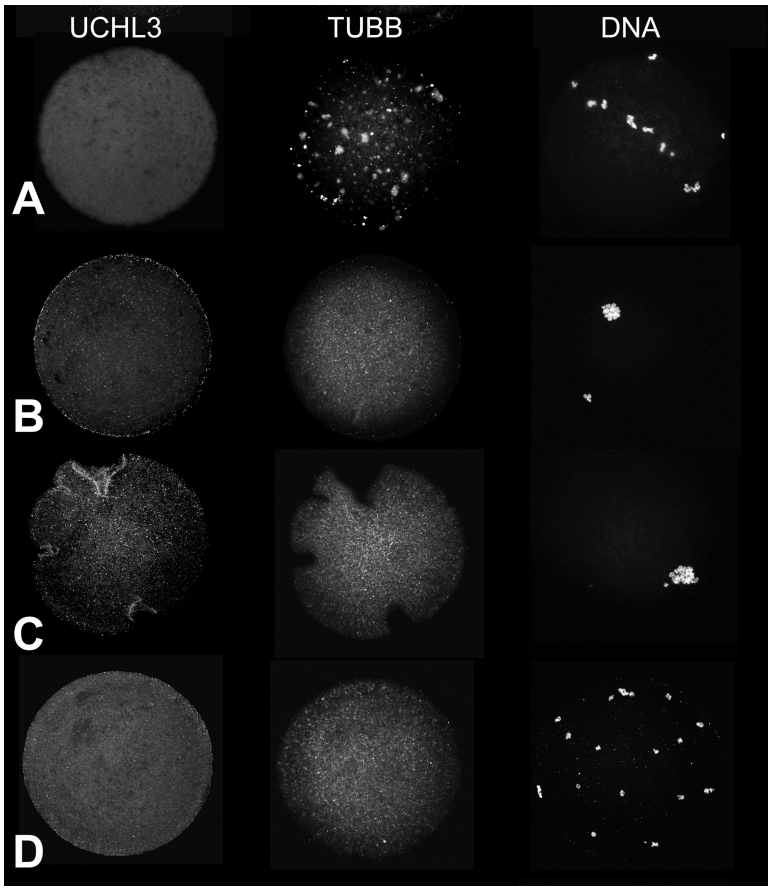

Fig. 3.

Dissipation of UCHL3 induced by **s**pindle microtubule (TUBB) depolymerization by nocodazole in the mouse oocytes**. A.** An oocyte treated with nocodazole at MII stage. **B, C.** Oocytes matured *in vitro* in the presence of nocodazole. Note the erosion of the oocyte surface in panel C. **D.** Similar to treatment at MII, some nocodazole-treated GV-oocyte displayed scattered chromosomes.

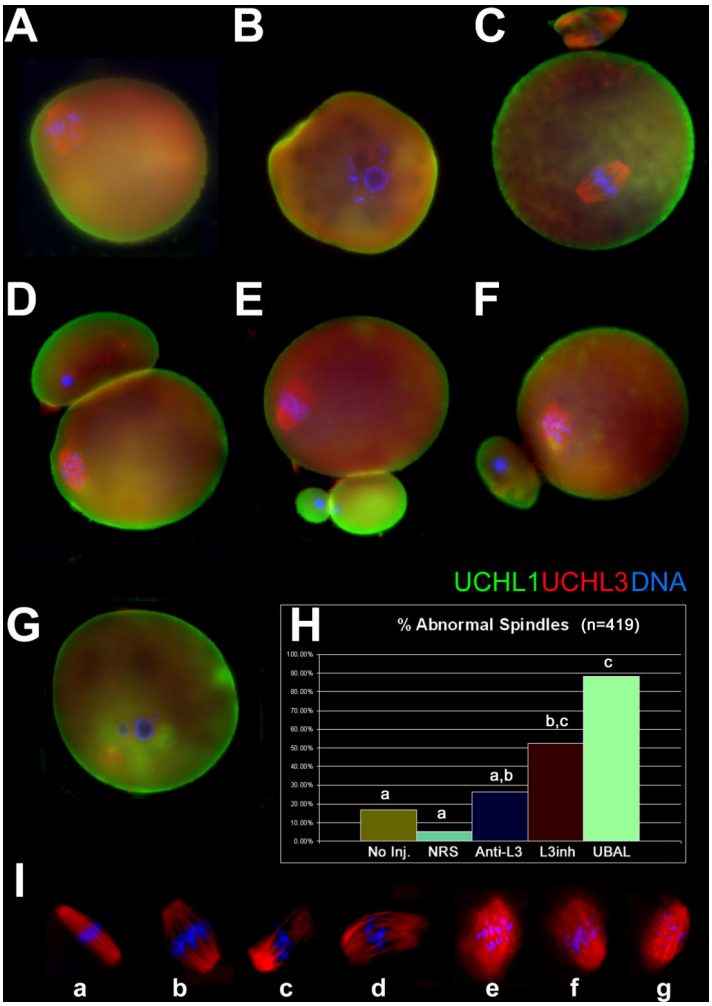

Fig. 4.

Mouse oocyte maturation is affected by the inhibition of oocyte ubiquitin C-terminal hydrolases. Oocytes were labeled with antibodies against UCHL1 (green) and UCHL3 (red); DNA was counterstained with DAPI. **A, B.** Oocyte matured in the presence of UCHL3 inhibitor showed increased incidence of abnormal metaphase-II spindles (**A**, note uneven chromosome distribution and wide spindle poles) or a failure to complete germinal vesicle breakdown (**B**; a large nucleolus precursor body typical of a GV-stage oocyte is present). **C.** Control oocyte with well focused spindle poles and a first polar body (PB1). **D-G.** Oocyte preinjected with UBAL showed abnormally large PB1 (**D**) or multiple PB1s (**E**), abnormal spindles with misaligned chromosomes (**D-F**), or premature chromatin condensation (PCC) following GVBD (**G**). **H.** Diagram of abnormal spindle frequencies in various UCHL3-affecting treatments shows average percentages of abnormal spindles from two replicates in mouse metaphase-II oocyte (n=419) that were injected at the GV-stage with ubiquitin-aldehyde (UBAL), affinity-purified rabbit antibody against UCHL3 (Anti-L3) or non-immune rabbit serum (NRS), or matured without preinjection (No Inj.), or without preinjection and in the presence of a specific inhibitor of UCHL3 (L3inh). **I.** Examples of

normal (**a, b**; control oocyte) and abnormal (**c-g**; UBAL-injected oocyte) metaphase II spindles and chromosomes from this trial.

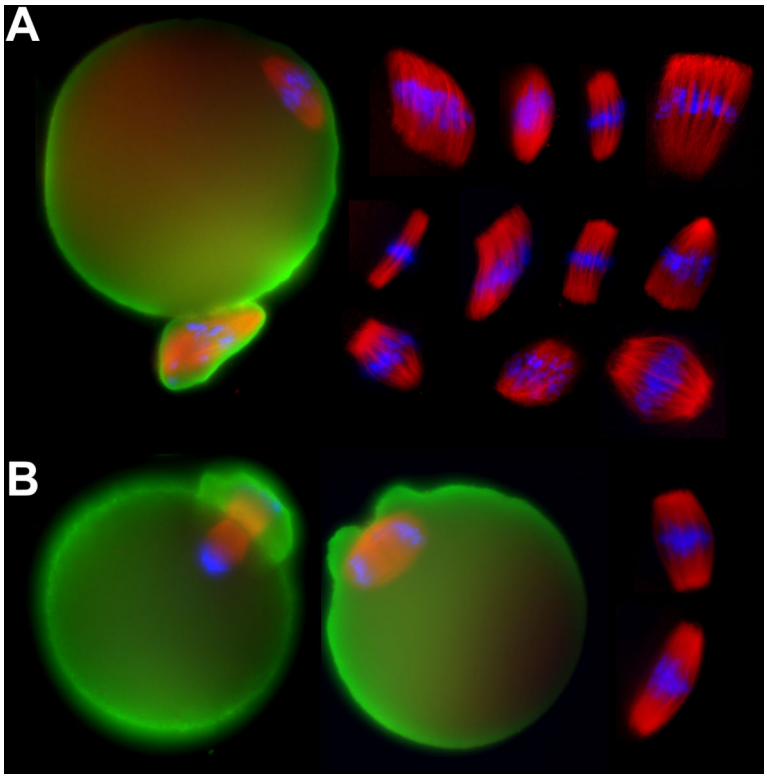

Fig. 5.

Metaphase II spindles in the oocyte injected with anti-UCHL3-antibody or non-immune rabbit serum (NRS) at GV stage, and processed 16 h later for immunofluorescence with antibodies against UCHL1 (green) and UCHL3 (red), combined with DNA stain DAPI (blue). **A.** Oocyte injected with a rabbit anti-UCHL3 antibody prior to IVM show various abnormalities such as lack of pole microtubule focusing, very narrow or very wide spindles and disarrayed metaphase chromosome plates. Note the presence of a second spindle pole within the polar body of an oocyte shown on the left. **B.** Control oocyte injected at GV-stage with non-immune rabbit serum show focused spindle poles even in cases where they did not reach metaphase II after 16 hours of IVM.

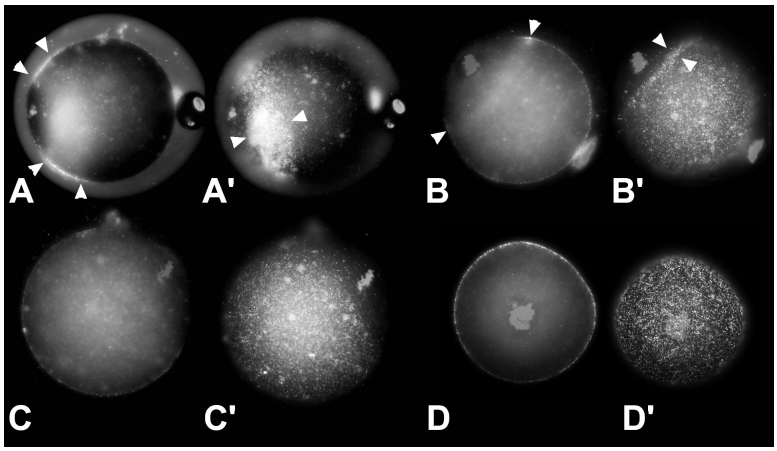

Fig. 6.

Pre-injection of MII-oocytes with UBAL alters cortical granule distribution during subsequent culture for 6 h. CGs were labeled with green fluorescent lectin LCA-FITC. DNA was counterstained with DAPI. Each oocyte is shown in equatorial (**A-D**) and surface (**A'-D'**) plane. After 6 h of culture, the MII oocyte preinjected with UBAL (**A, A', B, B'**) showed a distinct collar-like aggregation (arrowheads) of CGs adjacent to the CG-free area containing the oocyte spindle. Such a CG pattern was not present in control MII oocyte cultured for 6 hours (**C, C'**) or in oocyte matured in the presence of an inhibitor of UCHL3, which does not accumulate in the oocyte cortex (**D, D'**).

Table 1

Primers employed for obtaining cDNA probes

Gene Symbol	Forward primers 5′-3′	Reverse primers 5′-3′	GeneBank Accession number	Product size (bp)
Mouse *Uchl1*	GGGAGGTCCGCTTCTCTG	CTAGACAAACCACATCCAGGG	BC039177	309
Mouse *Uchl3*	GAGAGCCAAATTCCTGGAGA	TCTGTCAAGATGCTATGCCG	BC048481	307
Human *UCHL1*	CCAGTTCAGAGGACACCCTG	ACACTGGGGAGAATGCTTCA	NM_004181	345
Human *UCHL3*	CTGTGTCAATGAGCCCTGAA	GCTATGCTGCAGAAAGAGCA	NM_006002	318

TABLE 2

	Treatment	Replicates	N-oocyte treated	Key parameter-treatment group	Key parameter-control group	Main outcome & conclusion
A	UCHL3-inhibitor present during IVM	2	215	52.6 ± 4.8% had abnormal/missing spindles	16.9 ± 13.1% had abnormal/missing spindles	Abnormal oocyte maturation with defective spindles ***Conclusion:*** UCHL3 plays a role in spindle formation/function during IVM.
B	UBAL injection in GV oocyte & subsequent IVM	2	182	32 % metaphase II UBAL-oocytes after 16 h of IVM; 88.3±11.8% had abnormal spindles;	88% MII-oocytes After 16 h IVM; 5.1±0.6% sham injected oocytes had abnormal spindles (P=0.02)	Maturation to metaphase II reduced to 37 % of control; defective spindles, failed GVBD/metaphase I plate formation, abnormally large PB1. ***Conclusion:*** UCHs are important for oocyte maturation
C	Anti-UCHL3 AB injection at GV & IVM	2	172	in L3AB oocyte: 53.6 ± 3.7 μn); (P=0.004)	Spindle pole width in control oocyte: 39.0 ± 2.1 μm	Widened spindle poles observed; % of morphologically abnormal spindles not significantly different from control. ***Conclusion:*** UCHL3 plays a role in spindle formation/spindle pole focusing
		6	569			

ABBREVIATIONS

GV-germinal vesicle oocyte

GVBD-germinal vesicle breakdown

IVM-in vitro maturation

MII-metaphase II-oocyte

L1AB-mouse antibody against UCHL1 (ab20559, Abcam, Cambridge, MA)

L3i-inhibitor of UCHL3 (EMD/Calbiochem, Gibbstown, NJ: Cat # 662069)